The second magnetization peak and the peak effect phenomenon in the superconductor $Ca_3Rh_4Sn_{13}$

S. Sarkar [a,*], P.L. Paulose [a], S. Ramakrishnan [a], A.K. Grover [a], C.V. Tomy [b], G. Balakrishnan [c], D.McK. Paul [c]

[a] *Department of Condensed Matter Physics and Materials Science, Tata Institute of Fundamental Research, Colaba, Mumbai 400005, India*

[b] *Department of Physics, Indian Institute of Technology, Powai, Mumbai 400076, India*

[c] *Department of Physics, University of Warwick, Coventry CV4 7AL, UK*

Abstract

We report on the observation of the anomalous second magnetization peak (SMP) and the peak effect (PE) in juxtaposition to each other in the isothermal magnetization hysteresis loops at $T \leqslant 4$ K in a weakly pinned single crystal of an isotropic superconductor $Ca_3Rh_4Sn_{13}$ ($T_c \approx 8.2$ K). The position of the SMP does not display any temperature variation, whereas the PE appearing at the edge of the irreversibility line progressively moves towards lower fields as temperature increases. At $T \approx 5$ K, the PE nearly swamps the SMP, and above this temperature only the PE can be observed. If the SMP and the PE can be construed as representing changes in the spatial order of the flux line lattice (FLL), the apparent merger of loci of the peak fields of the SMP and the PE in the neighborhood of $H \approx 15$ kOe at a reduced temperature t $[= T/T_c(0)]$ of about 0.6 could imply the existence of a multi-critical point.

Keywords: Second magnetization peak; Peak effect; Multi-critical point; Minor hysteresis curve; Metastability; $Ca_3Rh_4Sn_{13}$

1. Introduction

The renaissance of interest in the *vortex matter* studies since the advent of high T_c superconductors stems from a variety of novel phases and the transformations amongst them due to the competition and interplay between interaction, disorder and thermal fluctuations [1]. The effect of pinning by static random impurities on an ideal flux line lattice (FLL) compromises its perfect long-range translational order but imparts an electrical current carrying capacity to the vortex array with minimal loss [2]. Thermally activated vortex creep can lead to the temporal decay of this critical current density J_c. The critical current of a superconductor is usually expected to decrease with the increase in either the temperature (T) or the magnetic field (H). It is thus considered anomalous to often encounter in real systems a non-monotonic behavior in J_c, designated either as a peak effect (PE) or as a fishtail effect (FE) [2,3]. A priori, the

PE and the FE are two distinct mutually exclusive anomalies in J_c, as they are usually observed in two different regimes of the thermomagnetic (H, T) phase space. The FE (also referred to as the second magnetization peak (SMP)), which has been ubiquitously observed in high T_c cuprates [3–8], refers to a characteristic shape of the isothermal dc magnetization hysteresis loop. The PE phenomenon on the other hand relates to a sharp anomalous increase/upturn in J_c, while approaching the superconductor-normal phase boundary [9,10]. It is widely accepted [11] that the PE signals an abrupt softening of the elastic modulii (essentially the shear modulus c_{66}) of the vortex solid, which in turn can get pinned more strongly by the underlying quenched random inhomogeneities. In weakly pinned crystals, the PE manifests itself either in juxtaposition to a sharp resistive kink [12,13] or is accompanied by a jump in equilibrium magnetization (entropy) amounting to a calorimetric anomaly [14–16], all of which can be attributed to the first order nature of a transition accompanying the PE. Hence, the PE can be argued as a FLL melting or FLL amorphization transition such that no long range translational or orientational correlation order survives [11,17–19] in the lattice.

On the other hand, the FE (or SMP), which occurs in a field interval well below the upper critical field H_{c2}, is broadly considered to be disorder induced [3–5]. However, there exists much debate about the origin of this phenomenon and its underlying mechanism in the context of experimental results in a variety of high T_c superconductors. Three decades ago [20], the SMP was believed to be originating generally in the disordered superconductors having two component response such that one of the components with a lower T_c (and H_{c2}) acts as a source of additional pinning for the other component as the field is increased beyond its H_{c2} in an isothermal scan. After the advent of high T_c superconductors, the newer explanations for the anomalous variations in J_c analogous to the SMP have been based on a whole variety of reasonings, such as, (i) the presence of weaker superconducting regions to matching effects of oxygen deficient structures (in systems like $YBa_2Cu_3O_{7-\delta}$) [21], (ii) the collective creep phenomenon [22,23], (iii) the surface barrier effect [24], (iv) a thermomagnetic instability related to the shape and size of the sample [25], (v) the local fluctuations in J_c persisting on mesoscopic length scales [26], (vi) the injection (and coexistence) of disordered regions with ordered regions [27], etc. *Prima facie*, the physical basis of the anomalous variations in J_c, *a la* the SMP and the PE phenomena, are discussed in different terms. There are only a few reports in the literature on high T_c superconductors, where the presence of the two distinctly different anomalous variations in J_c can be claimed to be evident [5,7]. The issues related to a clear distinction and the possible connection(s) between the PE and the SMP, therefore, remain open.

Recently, we have reported [28] the details of the PE phenomenon in a weakly pinned single crystal of an isotropic low T_c superconductor $Ca_3Rh_4Sn_{13}$ ($T_c(0) \approx 8.2$ K), investigated via dc magnetization experiments using a SQUID magnetometer and the ac susceptibility measurements. It was shown that the PE regime in this system comprised two discontinuous, first-order-like transitions located near its onset and peak positions, in accordance [17] with a stepwise amorphization/pulverization of the FLL. On further extending the dc magnetization measurements down to lower temperatures and higher fields, we have now discovered the presence of the two anomalous variations in J_c in juxtaposition to each other over a large part of the (H, T) phase space in a given isothermal hysteresis scan. In this paper, we present the new results pertaining to the observation of the SMP and the quintessential PE phenomenon in $Ca_3Rh_4Sn_{13}$. The field window across which the fishtail like feature occurs remains almost invariant with temperature, whereas the PE hysteresis bubble shifts to lower fields along with the upper critical field H_{c2} as the temperature increases. At higher temperatures ($T \geqslant 4.8$ K), the PE overlaps with the SMP and the latter cannot be identified distinctly. Thermomagnetic history dependence of J_c reveals different dynamics and pinning mechanisms associated with these two effects. Finally, a modified phase diagram can be constructed where several glassy phases, like, the Bragg glass, the vortex glass, the shattered glass, the pinned amorphous and the unpinned

amorphous phase, can be marked/identified. These results not only elucidate the distinction between the SMP and the PE, but also focus onto the circumstances in which the loci of field-temperature (H, T) values, which mark the different characteristic features in the anomalous variations in J_c, get admixed to give the notion of the possible presence of a multi-critical point in the vortex phase diagram.

2. The sample and the measurements

The crystal ($3.2 \times 3.1 \times 0.6$ mm^3, mass = 48.1 mg) of $Ca_3Rh_4Sn_{13}$ used for the present experiments is the same that was used in our earlier [28,29] studies. It has a rather narrow critical fluctuation region in the (H, T) phase space, as inferred from the Ginzburg number G_i ($\sim 10^{-7}$) [1], which is several orders of magnitude lower than the corresponding values in high T_c cuprates ($G_i \sim 10^{-2}$). The smallness of G_i indicates the narrowness of the region [1] in which thermal fluctuation effects can be significant in $Ca_3Rh_4Sn_{13}$. In addition, the relatively small value of the J_c/J_0 ratio ($\sim 10^{-4}$) in single crystals of this compound, where J_c and J_0 are the depinning and depairing current densities, respectively, classifies such superconducting samples to be weakly pinned. The weak pinning scenario is extremely helpful as the pinned state of the FLL can be studied under the realm of Larkin–Ovchinnikov [30,31] collective pinning theory. The dc magnetization was measured on a 12 T vibrating sample magnetometer (VSM) (Oxford Instruments, UK). The dc field was swept at several rates ranging from 1.2 to 0.05 T/min, while recording the magnetization hysteresis loops at various fixed temperatures.

3. Experimental results

3.1. Identification of the SMP and the PE from isothermal dc magnetization measurements

The main panel in Fig. 1 shows the isothermal dc magnetization hysteresis loop for $Ca_3Rh_4Sn_{13}$ at 1.7 K obtained by sweeping the magnetic field at a constant rate of 0.2 T/min. A superconductor attempts to shield itself from the changes in the external magnetic field by setting up macroscopic currents $J_c(H)$ which can be estimated from the width of the magnetization hysteresis using the Bean's critical state model (CSM) [32], such that $J_c(H) \propto [M_\downarrow(H) - M_\uparrow(H)]$ [33]. Here $M_\uparrow(H)$ and $M_\downarrow(H)$ represent the magnetization along the forward and reverse legs of the hysteresis loop, respectively. Thus, a non-monotonic behavior in J_c can reveal itself as an anomalous modulation in the width of the magnetization hysteresis loop. Such characteristic modulation features can be identified in the M–H loop, as shown in Fig. 1. The first anomalous modulation between H_{vg} and

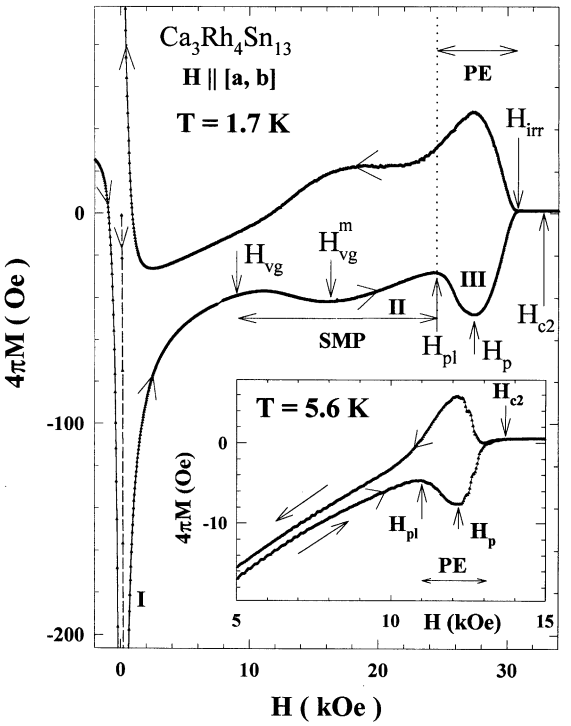

Fig. 1. The main panel shows the right half of the magnetization hysteresis loop ($H \| [0\,0\,1]$) recorded at 1.7 K in a single crystal of $Ca_3Rh_4Sn_{13}$. The initial protion of the M–H loop is shown as a dashed curve. The M–H loop comprises three peaks, marked I, II and III (see text for details). The two anomalous modulations in M–H loop are termed as the SMP and the PE. The inset shows a portion of the M–H loop at 5.6 K, where only one anomalous modulation termed as the PE can be seen.

H_{vg}^{m} is located well below H_{c2}, whereas the second anomalous modulation is the so called peak effect bubble between H_{pl} and H_{irr} through H_p, located close to H_{c2}. In principle, the envelope hysteresis loop ($0 \leqslant H \leqslant H_{c2}$) displays three magnetization peaks (I–III). Following the nomenclature in literature, if the first anomalous modulation (peak II) is to be referred as the SMP, the second anomalous modulation (peak III) identifying the PE may be designated as the third magnetization peak. It may be pointed out that the two portions of the hysteresis loops pertaining to the second and third peaks are visibly asymmetric, i.e., the M–H curve along the reverse leg is not a mirror image of that on the forward leg in between the fields H_{vg} and H_p. We have marked the field positions corresponding to the maximum width of the SMP hump as H_{vg}^{m}. Above H_{vg}^{m}, the hysteresis width (and hence the macroscopic current J_c) decreases until it reaches the field H_{pl}, which is to be identified with the onset of the PE. The inset panel in Fig. 1 presents a portion of the magnetization hysteresis loop obtained at 5.6 K, which alludes to the presence of only one anomalous modulation in $J_c(H)$ located close to the H_{c2} and is therefore identified with the PE. The evolution of the SMP and the PE as a function of temperature is elucidated in Fig. 2(a)–(d), where the portions of the M–H loops are plotted for temperatures 1.7, 3.5, 4.32 and 6.1 K, respectively. The field window of the SMP, which appears well below H_{c2}, seems to be insensitive to the temperature variation. However, the PE shows a strong temperature dependence, in accordance with the results reported in

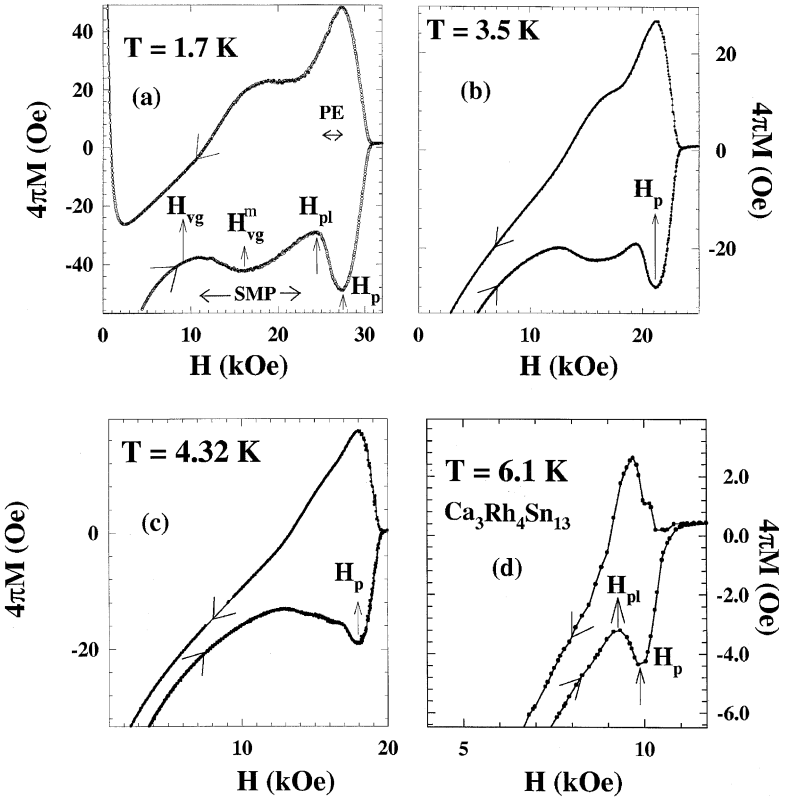

Fig. 2. Portions of the M–H loops at (a) 1.7 K, (b) 3.5 K, (c) 4.32 K and (d) 6.1 K in $Ca_3Rh_4Sn_{13}$, which focus on the temperature variations of the SMP and the PE. Note that at 4.32 K (panel c), one composite anomalous modulation encompassing the SMP and the PE is evident, whereas at 6.1 K (panel d), only the PE anomaly is observed.

our earlier studies [28]. A clear distinction between the SMP and the PE can be observed in our present measurements only up to a temperature of about 4 K, above which the field interval of the PE starts overlapping with that of the SMP (see M–H curve at $T = 4.32$ K in panel (c)). Above 5 K, only the PE can be observed. The span of PE shifts progressively to the lower fields with increase in temperature (cf. data at $T = 6.1$ K in panel (d)), until the PE anomaly eventually disappears at temperatures above 7.2 K (cf. Fig. 8).

3.2. Memory effect of J_c across the SMP and the PE

To explore the metastability effects in the SMP and the PE regions, we have examined the thermomagnetic path dependence of J_c by studying the characteristics of the minor hysteresis loops vis a vis the envelope hysteresis loop [34–36]. In order to create different metastable states, the vortex state has been prepared in the ZFC and the FC modes. For the ZFC mode, sample was cooled down to the lowest temperature in zero magnetic field and the magnetization was measured while ramping the magnetic field. In the FC mode, the magnetic field was first applied to the sample in the normal state. It was then cooled below T_c to the required temperature, after which the magnetization values were recorded by either increasing or decreasing the magnetic field. The magnetization curves so obtained at $T = 1.7$ K are illustrated in Fig. 3. The first interesting observation to note is that the minor magnetization curves initiated from the $M_{FC}(H)$ values (i.e., FC-minor curves), where H is less than the onset field of the SMP hump, H_{vg}, do not reach up to the envelope hysteresis loop, but remain less diamagnetic than the latter loop. This scenario changes as H approaches H_{vg}. Note that the rising part of the FC-minor curve overshoots the envelope loop, when the initial field H exceeds H_{vg}. The overshot FC-minor curves turn inwards and decay exponentially before eventually merging into the envelope loop. The characteristic overshooting feature, i.e., the differences between the magnetization values on the envelope curve and those on the portions of the FC-minor curves lying outside the envelope curve increase as H increases from H_{vg} to H_{pl}. Above H_{pl}, the observed

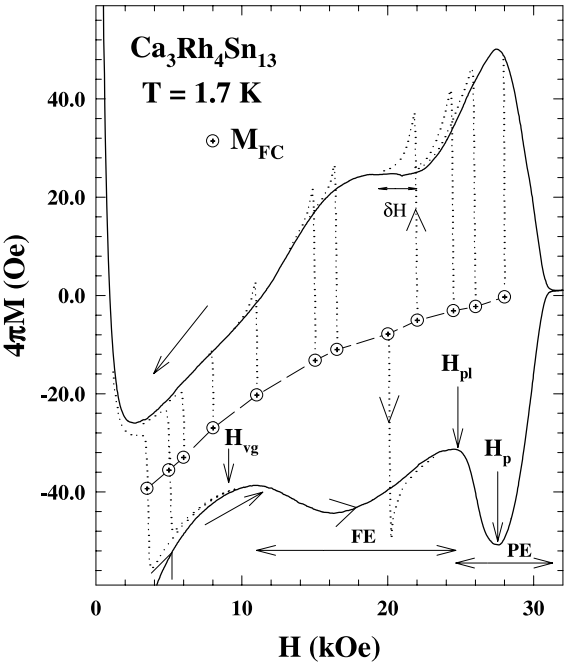

Fig. 3. The minor magnetization curves initiated from field cooled magnetization $M_{FC}(H)$ values lying in different regions of the entire field span at 1.7 K in $Ca_3Rh_4Sn_{13}$. The ZFC envelope loop is shown as a continuous line. Each of the FC minor curves initiated from $H_{vg} \leqslant H \leqslant H_p$ overshoots the envelope loop and reaches a saturated magnetization value, before rolling onto the envelope loop. The field interval δH required by a FC minor curve to reach upto the envelope loop is also indicated in one particular case.

difference decreases and eventually disappears near the peak field H_p of the PE.

Recalling that the width of the magnetization hysteresis loop correlates with the current density J_c via the Bean's CSM, the overshooting of the FC-minor curves implies that $J_c^{FC}(H) \geqslant J_c^{ZFC}(H)$ over the field interval $H_{vg} \leqslant H \leqslant H_p$, i.e., from the onset of the SMP up to the peak of the PE. Above H_p, all the metastability and the memory effects are expected to disappear [17,37–39], and hence the overshooting by the FC-minor curves ceases (cf. Fig. 3). Another interesting feature to note from Fig. 3 is the variation in δH as a function of H. δH is the field interval required by a FC-minor curve to merge into the ZFC envelope loop as a function of H. Although the extent of the overshooting by a FC-minor curve starts decreasing above H_{pl}, the

field change δH required to anneal a FC configuration of the vortex matter to the neighboring ZFC like state keeps on increasing well beyond H_{pl}. This interval δH appears to become negligibly small above H_p, where the history dependence in $J_c(H)$ disappears.

It is useful at this point to invoke the Larkin–Ovchinnikov collective pinning scenario [30,31] to characterize an interesting facet of the ZFC and FC states described above. Within the framework of collective pinning, J_c is given by the pinning force equation:

$$F_p = J_c H = (W/V_c)^{1/2} = [n_p \langle f_p^2 \rangle / R_c^2 L_c]^{1/2}, \qquad (1)$$

where W represents the pinning parameter, V_c is the correlation volume of a Larkin domain, n_p is the density of pinning centers (pins), f_p is the elementary pinning interaction and R_c and L_c are the collective pinning radial and longitudinal correlation lengths, respectively. The observation that $J_c^{FC}(H) \geqslant J_c^{ZFC}(H)$ for $H_{vg} \leqslant H \leqslant H_p$ implies that $V_c^{FC} \leqslant V_c^{ZFC}$, i.e., the FLL in the FC mode is more disordered with finely divided Larkin domains with lesser extent of lattice correlations (i.e., smaller values of R_c and L_c). However, below the onset field H_{vg} of the SMP, the inability of the FC-minor curve to reach upto the ZFC envelope curve could imply that the procedure of cooling in a field $H \leqslant H_{vg}$ creates a more ordered FLL having correlation volume even larger than that of the corresponding ZFC state (i.e., $J_c^{FC}(H) \leqslant J_c^{ZFC}(H)$ for $H \leqslant H_{vg}$). The situation that $J_c^{FC} \leqslant J_c^{ZFC}$ has been encountered in some of the weakly pinned crystals of $YBa_2Cu_3O_{7-\delta}$ [40,41] and $Bi_2Sr_2CaCu_2O_{8-\delta}$ [42].

3.3. ZFC minor curves

The envelope hysteresis loop comprises the magnetization curves generated by cycling the field between $\pm H_{max}$, where $H_{max} \geqslant H_{c2}$. As per the usual prescription of the CSM, in which one assumes $J_c(H)$ to be path independent, all minor curves that can be generated by reversing the field before reaching the normal state (i.e., by reversing from $H \leqslant H_{c2}$) should eventually overlap with the envelope curve. The deviations from such a behavior could further reflect the path dependence in $J_c(H)$, just as the inequality, $J_c^{ZFC} \neq J_c^{FC}$. We show in the main panel of Fig. 4 an entire family of minor curves generated by reversing the field from different points on the forward leg of the envelope curve. The following features emerge from an examination of these minor curves. The curves initiated from $H \leqslant H_{vg}$ readily merge into the reverse envelope curve, thereby upholding the prescription of the CSM. The minor curves initiated from $H_{vg} \leqslant H \leqslant H_{vg}^m$ do not reach up to the reverse envelope loop. However,the differences between the minor curves and the reverse envelope loop are rather small. The minor curves initiated from $H_{vg}^m \leqslant H < H_{pl}$ once again readily merge into the

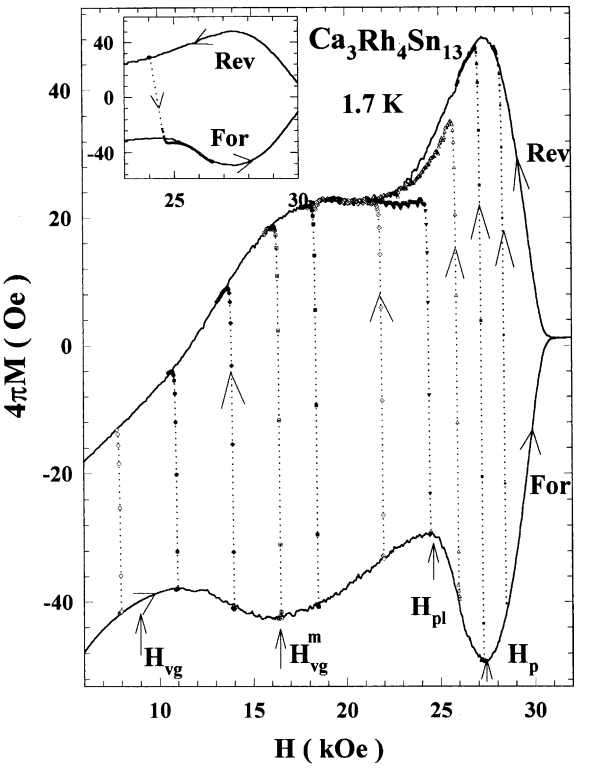

Fig. 4. The minor magnetization curves initiated from chosen fields lying on the forward leg of the envelope hysteresis loop at 1.7 K in $Ca_3Rh_4Sn_{13}$. The inset shows a minor curve initiated from a field value (near the onset position of the PE) lying on the reverse leg of the envelope loop. Note that the minor curves in the main panel fail to reach upto the envelope loop, whereas the minor curve in the inset panel overshoots the envelope loop.

reverse envelope loop. The feature of undershooting the reverse envelope loops resurfaces in a prominent manner for the minor curves initiated from $H_{pl} \leqslant H \leqslant H_p$. Finally, for $H \geqslant H_p$, the minor curves follow the path prescribed by the CSM, as all the features related to the history dependence in $J_c(H)$ disappear above the peak position of the PE [28].

The inset panel of Fig. 4 shows the feature of overshooting the forward envelope loop by a minor curve initiated from a field value lying near the onset position of the peak effect on the reverse leg. Kokkaliaris et al. [36] have recently argued that the experimental data of the minor hysteresis loops can be utilized to gain information about the plastic deformations in the collectively pinned elastic vortex solid across the region of the SMP in $YBa_2Cu_3O_{7-\delta}$. Their procedure relies on examining the differences in the saturated magnetization values (at given field values) belonging to the minor hysteresis loops initiated from the neighboring field values. It is asserted [36] that the extent of plasticity correlates with the difference in the magnetization values picked from successive minor curves. Keeping this in view, we have examined the differences in the saturated values of the neighboring minor curves generated from different points on the forward leg of the envelope curve in $Ca_3Rh_4Sn_{13}$. Fig. 5 shows the highest magnetization values of different minor curves (shown as filled triangles) along with the reverse envelope loop recorded at 1.7 K. The inset panel in Fig. 5 shows a plot of the differences in magnetization values (ΔM_{suc}) obtained from two successive minor curves as a function of those fields at which the said differences are ascertained. If the usual prescription of the CSM were to hold, the differences designated as ΔM_{suc} should vanish. The data in the inset panel of Fig. 5 shows that ΔM_{suc} values peak in between the onset and the peak positions of the SMP as well as those of the PE. It may be useful to recall here that the noise signal for the driven vortex matter maximizes between the onset and peak positions of the PE in $2H$-$NbSe_2$ [11]. The present data in $Ca_3Rh_4Sn_{13}$ could therefore be taken to support the notion of correspondence between the extent of plasticity and the accessibility of metastable states for the driven vortex

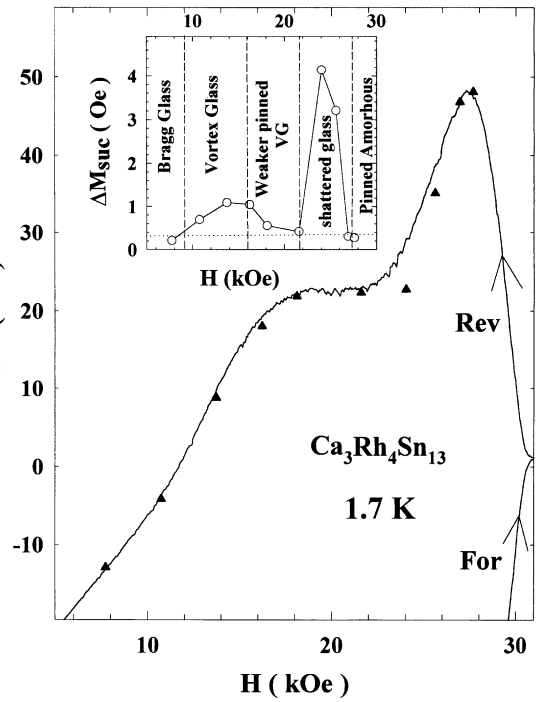

Fig. 5. The main panel shows the saturated values (filled triangles) of the minor curves initiated from chosen fields on the forward leg of the envelope loop. The continuous line represents the envelope loop. The inset panel shows the plot of the differences ($4\pi\Delta M_{suc}$) in magnetization values determined from the two neighboring (successive) minor curves versus the chosen fields at which such differences are ascertained. For a justification of the nomenclature of different regions in the inset panel, refer to Fig. 6.

matter between the onset and peak positions of the PE.

3.4. Identification of various glassy phases from the behavior of J_c

The width of the magnetization hysteresis loop directly provides a measure of the $J_c(H)$. Fig. 6 displays a log–log plot of $J_c(H)$ vs H at $T = 1.7$ K in $Ca_3Rh_4Sn_{13}$. On the basis of the differences in the characteristic behavior of J_c observed in different regions of the (H, T) phase space, the entire field span can be broadly subdivided into six parts, which have been designated as the small bundle pinning regime, the collective pinned elastic solid (power law regime), the vortex glass, the shattered

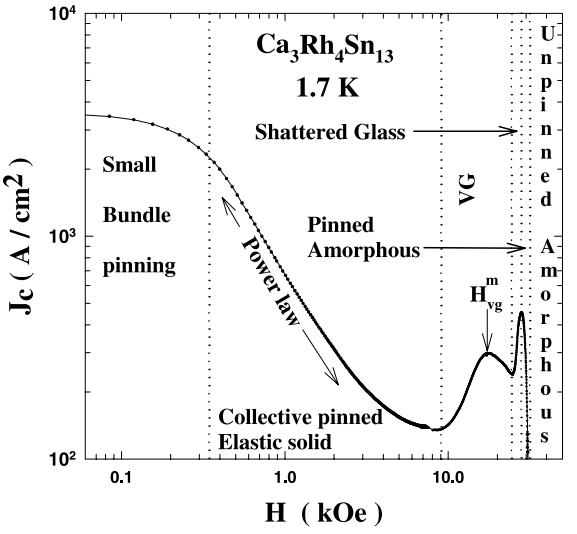

Fig. 6. Log–log plot of J_c vs H at 1.7 K in $Ca_3Rh_4Sn_{13}$. The two anomalous maxima in J_c lie in juxtaposition to each other. The entire field span has been demarcated into six regions (see text for details).

glass, the pinned amorphous and an unpinned amorphous. Of the various regions mentioned above, we first draw attention onto the collective pinned power law regime, which may be identified with the notion of the Bragg glass [43,44]. It is reasonable to consider that in this regime, vortex medium behaves as an elastic medium and the quasi-long range translational order prevails [43,44]. At fields below the lower end of this regime, the field dependence in $J_c(H)$ becomes weaker and it appears to approach a nearly field independent value expected for individually pinned vortices in the very dilute limit (i.e., when inter vortex spacing $a_0 \geqslant \lambda$, where λ is the penetration depth that measures the range of interaction between vortices). A crossover from an individually pinned (or a small bundle pinning regime) to a collectively pinned regime is to be anticipated at a threshold field H_{sb}, above which $J_c(H)$ follows the archetypal power law behavior. An order of magnitude estimate for H_{sb} can be made [1,45] in terms of the ratio J_c/J_0 ($\sim 10^{-4}$) and H_{c2} (~ 5 T) using the relation, $H_{sb} \sim 5[J_c/J_0]H_{c2}$, which gives H_{sb} as $\sim 10^{-2}$ T for $Ca_3Rh_4Sn_{13}$. Such an estimated value agrees well with the experimental value of H_{sb} (cf. Fig. 6).

Near the upper end of the power law regime in $J_c(H)$, the decay in $J_c(H)$ slows down, which effectively amounts to an onset of the enhancement effect of quenched random pins vis a vis interaction between the vortices. The first anomalous upturn in $J_c(H)$ could therefore be perceived as a transformation from a notionally elastic vortex state to a plastically deformed regime (vortex glass) in which topological defects, like dislocations, permeate in the ordered FLL [43,44]. As the dislocation density enhances between the onset (H_{vg}) and the peak (H^m_{vg}) positions of the SMP, the thermomagnetic history dependence in $J_c(H)$ becomes evident. Above H^m_{vg}, $J_c(H)$ starts to decay with the increase in H and the topologically defective FLL heals to some extent to a relatively weaker pinned vortex glass state as compared to that existing before H^m_{vg}.

The anomalous increase in $J_c(H)$ at the onset of the PE is accompanied by a significantly stronger manifestation of the path dependence in $J_c(H)$ (see inset panel in Fig. 5, which displays the peaking of δM_{suc} near H_p). Our earlier study of the PE phenomenon in $Ca_3Rh4_4Sn_{13}$ had revealed [28] that the entry into the PE regime in an isofield scan commences via a sudden shrinkage (i.e., fracturing of the vortex solid) of the correlation volume of the FLL. The shattered vortex glass state progresses towards the completely amorphous state in a stepwise manner. At H_p, where the second anomalous variation in $J_c(H)$ ceases, all manifestations of the path dependence in $J_c(H)$ disappear.

Above the peak position of the PE, where the vortex matter has presumably transformed to an amorphous yet pinned vortex state [28], $J_c(H)$ displays a rapid collapse of pinning with an increase in H in response to the core softening effects (presumably related to the divergence of coherence length ξ on approaching H_{c2}). An unpinned amorphous state therefore precedes the arrival of the upper critical field H_{c2}.

4. Discussion

It is useful to collate all the information on the field–temperature values approximately marking the different characteristic features evident in Figs.

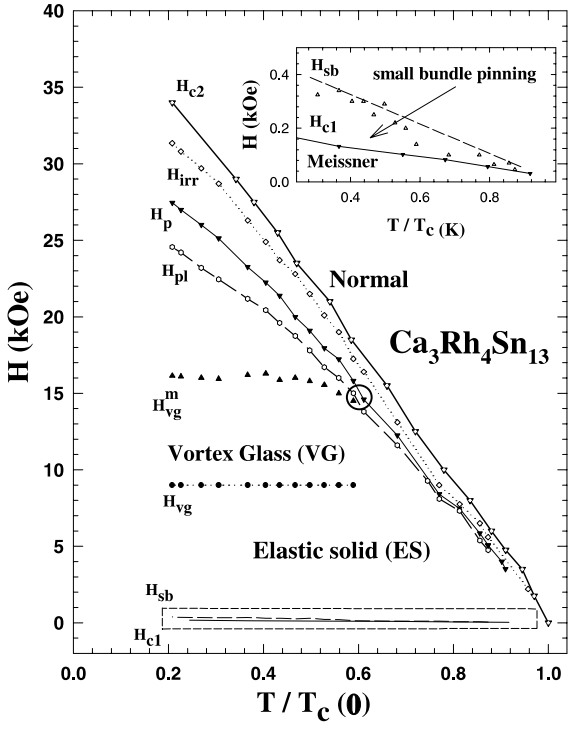

Fig. 7. A field–temperature diagram in which the temperature dependences of various characteristic features identifiable from J_c vs H plot as shown in Fig. 6 are indicated. For completeness purpose, the $H_{c1}(T)$ and $H_{c2}(T)$ lines determined in $Ca_3Rh_4Sn_{13}$ have also been marked. The inset panel shows the small bundle pinning regime lying in between the $H_{c1}(T)$ and $H_{sb}(T)$. The encircled region near $H \approx 15$ kOe and $T/T_c(0) \sim 0.6$ in the main panel identifies the pocket of notional multicritical point, where the two anomalous variations in $J_c(H)$ coalesce to yield only a single anomaly identifiable with the PE phenomenon.

1 to 6, and as described in the earlier sections. Fig. 7 represents the outcome of such an exercise in the form of a vortex classification diagram in the (H, T) space. At low temperatures (i.e., at $t \leqslant 0.6$, where $t = T/T_c(0)$), all the six regions as described in Section 3.4 can be identified in this diagram. In an isothermal scan, the first anomalous increase in $J_c(H)$ occurs across $H_{vg}(T)$, whereas the second anomalous variation commences across $H_{pl}(T)$. The $H_{pl}(T)$ values lie close to H_{c2} and follow the temperature dependence of the latter. Thus, $H_{pl}(T)$ decreases as T increases, whereas the $H^m_{vg}(T)$ values do not display such a variation. The difference between $H_{pl}(T)$ and $H^m_{vg}(T)$ decreases as t approaches 0.6 and the distinction between the two anomalous variations in $J_c(H)$ gets blurred in the magnetization curve. One therefore observes only a composite anomalous increase in $J_c(H)$ located at the edge of the irreversibility line $H_{irr}(T)$. $H_{irr}(T)$ represents the collapse of the pinning, a characteristic of the vortex matter while approaching the normal state boundary H_{c2}.

In a temperature scan, the anomalous increase in $J_c(T)$ just prior to the arrival of $T_{irr}(H)$, therefore, is intimately connected to the withering of the notion of the pinned vortex solid. Hence, the PE phenomenon finds a natural connection to the eventual collapse of the elastic modulii of the vortex solid. The first anomalous increase in $J_c(H)$, which amounts to a fishtail-like feature (SMP), thus requires a separate explanation in terms of the entities which are not strongly influenced by the thermal effects. It is, therefore, tempting to associate this anomaly with a pinning induced, dislocation mediated Bragg glass to vortex glass [43,44,46] transformation. The localized field-temperature region, where the resolution between the two anomalous variations in $J_c(H)$ ceases ($H \sim 15$ kOe, $t \sim 0.6$ in the phase diagram), may give the impression of a hypothetical multicritical point buried underneath (see the encircled region in Fig. 7). However, it may be reiterated that the PE phenomenon represents the continuity across this (underneath) region and tends to preclude the notion of a tricritical point in the neighbourhood of $H \sim 15$ kOe and $t \sim 0.6$.

The characteristics of the PE phenomenon in $Ca_3Rh_4Sn_{13}$ [11,28] are identical to those in the $2H$-$NbSe_2$ system [17], the detailed studies on which have provided ample evidence in favor of the assertion that the PE represents a first order transition related to the amorphization of the vortex matter in response to the collapse of the elastic modulii of the FLL. The $H_p(T)$ line therefore could be taken [1] to be the counterpart of the melting line of the pure FLL (in the absence of pinning). In $Ca_3Rh_4Sn_{13}$, the $H_p(T)$ line seems to extend down to $H \approx 3.5$ kOe. In the temperature scans, we had earlier reported [28] that the PE phenomenon could not be observed for the vortex lattices prepared at $H < 3.5$ kOe ($a_0 > 800$ Å). In the present experiments performed using a VSM,

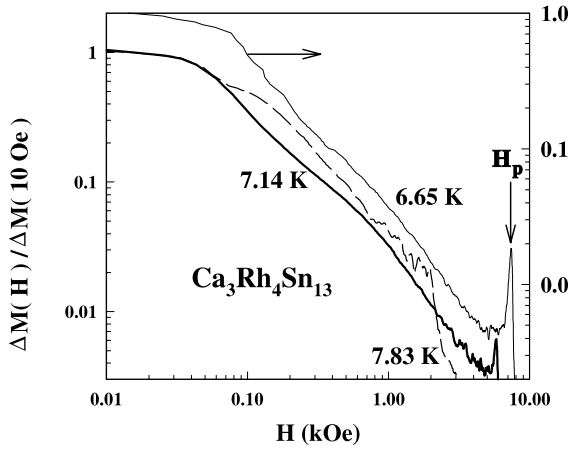

Fig. 8. Plot of normalized values of current density $[\propto \Delta M(H)/\Delta M(H = 10\ \text{Oe})]$ versus field at $T = 6.65$, 7.14 and 7.83 K, respectively in $Ca_3Rh_4Sn_{13}$. The y-scale for the curve at 6.65 K has been shifted up for clarity. Note that the hysteresis width at 7.83 K displays a sharp collapse near 2 kOe without yielding the PE feature.

we could observe an anomalous modulation in the M–H loops only upto $t = 0.94$. The width of the hysteresis loop collapses in a precipitous manner at $T = 7.83$ K ($t \approx 0.95$). Fig. 8 presents a comparison of (normalized) ΔM vs H data at $T = 6.65$, 7.14 and 7.83 K. The presence of the PE can be noted at the first two temperatures, whereas it is not evident at 7.83 K. The collapse of the pinning at 7.83 K occurs near $H = 2$ kOe. This field value lies in the power law region in Fig. 5 and the vortex state prepared at such a field at 1.7 K therefore is expected to be reasonably well ordered. The absence of any fingerprint of the PE in temperature scans at $H \approx 2.5$ kOe in the temperature dependent ac susceptibility data [28] therefore calls for a rational explanation. In this context, it may be worthwhile to record here that the attempts to detect any anomaly in the equilibrium magnetization in the M–T scans at $H =$ 3.0 kOe or in M–H scans at $t \geqslant 0.94$ did not yield any fruitful result, presumably due to limitations in the accuracy of the magnetization data obtained with the VSM. More experiments are desired to explore the temperature evolution of the vortex states prepared in the field range of 0.2–2 kOe in $Ca_3Rh_4Sn_{13}$. Vortex states prepared in the FC mode in this field range are more ordered than those created in the ZFC manner.

5. Summary

To summarize, we have presented new magnetization results in a weakly pinned single crystal of an isotropic superconductor $Ca_3Rh_4Sn_{13}$ at lower temperatures and higher fields using a VSM (as compared to the earlier studies [28,47]). The results help to clearly distinguish between the two anomalous variations in J_c which could be classified as the SMP and the PE, respectively. We have clearly shown the demarcation of the entire field span into different regions, where the said two anomalies are present in juxtaposition to each other in an isothermal scan. The evolution in the two anomalies with temperature has been studied and their relationship with the notion of the multicritical point in the thermomagnetic (H, T) diagram of the vortex matter has been indicated.

Acknowledgements

We would like to gratefully acknowledge continuous discussions with all our collaborators on vortex state studies, especially, S.S. Banerjee, S. Bhattacharya, M. Chandran, T.V. Chandrashekar Rao, P.K. Mishra, G. Ravikumar, V.C. Sahni, and A.A. Tulapurkar. The Warwick group acknowledges EPSRC for their research grant. This work formed a part of the invited talk given by one of us (A.K.G.) at "The Joint Vortex Physics and ESF-Vortex Matter Workshop" held at Lunteren, The Netherlands from August 27–September 1, 2000.

References

[1] G. Blatter, M.V. Feigel'man, V.B. Geshkenbein, A.I. Larkin, V.M. Vinokur, Rev. Mod. Phys. 66 (1994) 1125, and references therein.
[2] M. Tinkham, Introduction to Superconductivity, McGraw-Hill, New York, 1996.
[3] M. Daeumling, J.M. Seuntjens, D.D. Larbalestier, Nature (London) 346 (1990) 332.

[4] E. Zeldov, D. Majer, M. Konczykowski, V.B. Geshkenbein, V.M. Vinokur, H. Shtrikman, Nature (London) 375 (1995) 373.
[5] K. Deligiannis, P.A.J. de Groot, M. Oussena, S. Pinfold, R. Langan, R. Gagnon, L. Taillefer, Phys. Rev. Lett. 79 (1997) 2121.
[6] H. Küpfer, Th. Wolf, C. Lessing, A.A. Zhukov, X. Lanon, R. Meier-Hirman, W. Schauer, H. Wühl, Phys. Rev. B 58 (1998) 2886, and references therein.
[7] T. Nishizaki, N. Kobayashi, Supercond. Sci. Technol. 13 (2000) 1, and references therein.
[8] D. Giller, A. Shaulov, R. Prozorov, Y. Abulafia, Y. Wolfus, L. Burlachkov, Y. Yeshurun, E. Zeldov, V.M. Vinokur, J.L. Peng, R.L. Greene, Phys. Rev. Lett. 79 (1997) 2542.
[9] A.B. Pippard, Philos. Mag. 19 (1969) 217.
[10] P.W. Anderson, Basic Notions in Condensed Matter Physics, Addison-Wesley, New York, 1983.
[11] M.J. Higgins, S. Bhattacharya, Physica C 257 (1996) 232, and references therein.
[12] H. Safar, P. Gammel, D.A. Huse, D.J. Bishop, W.C. Lee, J. Giapintzakis, D.M. Ginsberg, Phys. Rev. Lett. 69 (1992) 824.
[13] H. Safar, P.L. Gammel, D.A. Huse, G.B. Alers, D.J. Bishop, W.C. Lee, J. Giapintzakis, D.M. Ginsberg, Phys. Rev. B 52 (1995) 6211.
[14] A. Schilling, R.A. Fisher, N.E. Phillips, U. Welp, D. Dasgupta, W.K. Kwok, G.W. Crabtree, Nature (London) 382 (1996) 791.
[15] T. Ishida, K. Okuda, H. Asaoka, Phys. Rev. B 56 (1997) 5128.
[16] G. Ravikumar, P.K. Mishra, V.C. Sahni, S.S. Banerjee, S. Ramakrishnan, A.K. Grover, P.L. Gammel, D.J. Bishop, E. Bucher, M.J. Higgins, S. Bhattacharya, Physica C 322 (1999) 145.
[17] S.S. Banerjee, N.G. Patil, S. Saha, S. Ramakrishnan, A.K. Grover, S. Bhattacharya, G. Ravikumar, P.K. Mishra, T.V.C. Rao, V.C. Sahni, M.J. Higgins, E. Yamamoto, Y. Haga, M. Hedo, Y. Inada, Y. Onuki, Phys. Rev. B 58 (1998) 995.
[18] P.L. Gammel, U. Yaron, A.P. Ramirez, D.J. Bishop, A.M. Chang, R. Ruel, L.N. Pfeiffer, E. Bucher, Phys. Rev. Lett. 80 (1998) 833.
[19] X.S. Ling et al., Phys. Rev. Lett. 86 (2001) 712.
[20] A.M. Campbell, J.E. Evetts, Adv. Phys. 21 (1972) 327, and references therein.
[21] A.A. Zhukov, H. Küpfer, H. Claus, H. Wühl, M. Kläser, G. Müller-Vogt, Phys. Rev. B 52 (1995) R9871.
[22] L. Krusin-Elbaum, L. Civale, V.M. Vinokur, F. Holtzberg, Phys. Rev. Lett. 69 (1992) 2280.
[23] H. Safar, P.L. Gammel, D.J. Bishop, D.B. Mitzi, A. Kapitulnik, Phys. Rev. Lett. 68 (1992) 2672.
[24] D.T. Fuchs, E. Zeldov, M. Rappaport, T. Tamegai, S. Ooi, H. Shtrikman, Nature (London) 391 (1998) 373.
[25] Y. Kopelevich, P. Esquinazi, J. Low Temp. Phys. 113 (1998) 1.
[26] A. Gurevich, V.M. Vinokur, Phys. Rev. Lett. 83 (1999) 3037.
[27] C.J. van der Beek, S. Colson, M.V. Indenbom, M. Konczykowski, Phys. Rev. Lett. 332 (2000) 219.
[28] S. Sarkar, D. Pal, S.S. Banerjee, S. Ramakrishnan, A.K. Grover, C.V. Tomy, G. Ravikumar, P.K. Mishra, V.C. Sahni, G. Balakrishnan, D. McK. Paul, S. Bhattacharya, Phys. Rev. B 61 (2000) 12394.
[29] C.V. Tomy, G. Balakrishnan, D. Mck. Paul, Phys. Rev. B 56 (1997) 8346.
[30] A.I. Larkin, Yu.N. Ovchinnikov, J. Low Temp. Phys. 34 (1979) 409.
[31] A.I. Larkin, Yu.N. Ovchinnikov, Sov. Phys. JETP 38 (1974) 854.
[32] C.P. Bean, Rev. Mod. Phys. 36 (1964) 31.
[33] W.A. Fietz, W.W. Webb, Phys. Rev. 178 (1969) 657.
[34] S.B. Roy, P. Chaddah, J. Phys. Cond. Matt. 9 (1997) L625.
[35] G. Ravikumar, P.K. Mishra, V.C. Sahni, S.S. Banerjee, A.K. Grover, S. Ramakrishnan, P.L. Gammel, D.J. Bishop, E. Bucher, M.J. Higgins, S. Bhattacharya, Phys. Rev. B 61 (2000) 12490, and references therein.
[36] S. Kokkaliaris, P.A.J. deGroot, S.N. Gordeev, A.A. Zhukov, R. Gagnon, L. Taillefer, Phys. Rev. Lett. 82 (1999) 5116.
[37] W. Henderson, E.Y. Anderi, M.J. Higgins, S. Bhattacharya, Phys. Rev. Lett. 77 (1999) 2077.
[38] W. Henderson, E.Y. Anderi, M.J. Higgins, S. Bhattacharya, Phys. Rev. Lett. 80 (1998) 381.
[39] G. Ravikumar, K.P. Bhagwat, V.C. Sahni, A.K. Grover, S. Ramakrishnan, S. Bhattacharya, Phys. Rev. B 61 (2000) R6479.
[40] D. Pal, D. Dasgupta, B.K. Sarma, S. Bhattacharya, S. Ramakrishnan, A.K. Grover, 62 (2000) 669.
[41] S.O. Valenzuela, V. Bekeris, Phys. Rev. Lett. 84 (2000) 4200.
[42] S. Sarkar et al., unpublished.
[43] T. Giamarchi, P.Le. Doussal, Phys. Rev. Lett. 72 (1994) 1530.
[44] T. Giamarchi, P.Le. Doussal, Phys. Rev. B 52 (1995) 242.
[45] M.V. Marchevsky, Ph.D. Thesis, University of Leiden, The Netharlands, 1997.
[46] M.J.P. Gingras, D.A. Huse, Phys. Rev. B 53 (1996) 1519.
[47] S. Sarkar, S.S. Banerjee, A.K. Grover, S. Ramakrishnan, S. Bhattacharya, G. Ravikumar, P.K. Mishra, V.C. Sahni, C.V. Tomy, G. Balakrishnan, D. McK. Paul, M.J. Higgins, Physica C 341–348 (2000) 1085.